

# ADVANCEMENT AND APPLICATION OF BUBBLE DETECTOR TECHNOLOGY\*

M. A. Buckner, W. H. Casson and C. S. Sims  
Oak Ridge National Laboratory

## INTRODUCTION

Every field is searching for its better mouse trap, and the field of dosimetry is no different. Until recently, a dosimetrist would have been hard-pressed to identify an affordable and yet reliably accurate dosimeter for mixed neutron and gamma fields. A new technology has reared its head and is vying for position in the dosimetry community. This relatively young technology is building upon the foundation of the bubble chamber, conceptualized by Glaser in 1952 (Glaser 1952). Although the attitudes surrounding this technology, as with any new development, are somewhat mixed, with the proper combination of tweaking and innovative thought, applications of this technology hold great promise for the future of neutron dosimetry.

The Dosimetry Applications Research (DOSAR) facility of Oak Ridge National Laboratory (ORNL) is looking into some innovative applications of this technology. We are investigating options for overcoming its limiting features in hopes of achieving an unprecedented level of proficiency in neutron detection. Among these are the developing and testing of a Combination Area Neutron Spectrometer, CANS, assessing the plausibility of extremity applications, the assembly of an alternative reader for research, investigation of temperature-related effects and how to correct for them and considerations on the coming of age of neutron dosimetry via real time detection of bubble formation in Bubble Technology Industries Inc. (BTI) detectors.

In the space allowed, we will attempt to answer the questions: 1) What areas hold the greatest promise for application of this emerging technology?; 2) What obstacles must be overcome before full-blown application becomes a reality?; and 3) What might the future hold?

## PROMISING APPLICATIONS

The areas that hold the greatest promise for application of this technology are personnel neutron dosimetry, extremity neutron dosimetry and neutron spectrometry. Let us consider each of these briefly.

### Personnel Neutron Dosimetry

The BD-100R of BTI and Apfel Enterprises ( $\mathcal{A}$ ) Neutrometer exhibits energy response characteristics which are near dose equivalent, i.e., similar in shape to the fluence-to-dose equivalent conversion curve described in the International Commission on Radiological Protection Publication Number 21 (ICRP 21 h<sub>4</sub>) (ICRP 21 1973). Both of these devices provide the individual wearing them with an immediate visual indication of neutron irradiation, the BD-100R via the number of bubbles and the Neutrometer via displacement of a plunger or disc. Used in this capacity, they would be excellent for keeping neutron exposures As Low As Reasonably Achievable, ALARA. This passive attribute of their operation is considered by some as a highly desirable feature.

The convenience of having accurate neutron dose equivalent information at your fingertips; what bliss that would be! The acoustical vibration which accompanies a nucleation event, i.e., the pop associated with bubble formation, makes the active detection of bubble formation possible. This feature is, at present, only available in the new survey meter (ASM) and area monitor (AAM) from  $\mathcal{A}$ , both of which are second generation test versions and cost \$2395 and \$3395 respectively. But, alternative real-time acoustical processing,

\* Research sponsored by the Office of Health, U. S. Department of Energy under Contract No. DE-AC05-84OR21400 with Martin Marietta Energy Systems, Inc.

ARAP, is currently under development at DOSAR. This methodology will enable the BTI detectors to become active devices while maintaining a passive, fail-safe capacity, via optical counting of the bubbles should the electronics fail.

### Extremity Neutron Dosimetry

The difficulties associated with performing neutron dosimetry for the extremities stems fundamentally from the energy response characteristics of the devices used, typically TLD-600. The response of TLD-600 is at its maximum at thermal energies and decreases in a manner proportional to the inverse of the neutron velocity. This weakness is somewhat avoided in whole body dosimetry by relying on the inherent nature of the hydrogenous tissue of the body to reflect higher energy neutrons back into the device at lower, more readily detectable energies, i.e, in the albedo dosimeter. The lack of hydrogenous material in the extremities means that, for most neutron spectra, the signal to dose equivalent ratio for TLD-600 is very low.

Because bubble detectors (BD) are direct interaction devices possessing a near dose equivalent response whether in air or on a phantom, i.e., they are not dependent upon albedo neutrons, they circumvent the previous problem of the lack of hydrogenous tissue in the extremity. This would, in effect, enable the detection of a neutron dose to the extremities significantly lower than previously achievable with TLD-600. An extremity monitoring test using small vials of BD-100R material (PM-100) is slated for ORNL's Radiochemical Engineering Development Center (REDC) in the near future.

### Neutron Spectrometry

The current methods of obtaining neutron spectral information utilize equipment that is often bulky, expensive to obtain, and requires complex deconvolution algorithms to unfold the spectrum. This information is indispensable for performing accurate neutron dosimetry. Yet, most of these devices, specifically the Tissue Equivalent Proportional Counter (TEPC), NE-213, Rotational Spectrometer (ROSPEC) and  $^3\text{He}$ , share an alarming response trait. That common trait is their inability to effectively measure neutrons below 100 keV. When confronted with this deficiency, the reply is usually that very little of the dose comes from neutrons below this energy; therefore, the fluence in this region may be ignored. At even 100 keV there is about a factor of 6 difference in the  $h_v$  between 100 keV and 10 keV ( $0.579 \times 10^{-5}$  mrem-cm<sup>2</sup> compared to  $0.099 \times 10^{-5}$  mrem-cm<sup>2</sup>). This is very troubling considering, for TLD users, the majority of their signal comes from neutrons below 100 keV. Therefore, such an oversight could have far-reaching effects on the quality of neutron dosimetry in the field. In a power reactor environment, neglecting neutrons below 100 keV would be inappropriate. But how can one practically obtain a measure of the fluence below 100 keV?

Possibly the most exciting application of bubble detector technology lies in the area of neutron spectrometry. The Combination Personnel Neutron Dosimeter (CPND) has demonstrated that a high degree of accuracy in measuring the neutron dose equivalent and spectra is attainable through the combination of TLD and BD technology. Measurements were taken of five *insitu* work environments and five radioisotopic source spectra to assess the capabilities of this technique. The source irradiations,  $^{238}\text{PuBe}$ ,  $^{252}\text{Cf}$  moderated by polyethylene and  $\text{D}_2\text{O}$  ( $^{252}\text{Cf}_{(\text{PE})}$  and  $^{252}\text{Cf}_{(\text{D}_2\text{O})}$ ), a mixture of  $^{252}\text{Cf}_{(\text{D}_2\text{O})}$  and  $^{238}\text{PuBe}$  (MIX(2)), and a mixture of  $^{252}\text{Cf}_{(\text{PE})}$ ,  $^{252}\text{Cf}_{(\text{D}_2\text{O})}$  and  $^{238}\text{PuBe}$  (MIX(3)), were performed at the Radiation Calibration Laboratory (RADCAL), and the *insitu* measurements were taken at five selected locations at REDC. The measured results for total neutron dose equivalent were within 11% for the *insitu* tests and within 2% for the source irradiations as compared to reference values obtained from spectra published in the literature (Block et al. 1967; ISO/DIS 1986) or from Bonner multi-sphere (BMS) measurements (Liu et al. 1989). Presented in Figures 1 and 2 are the neutron dose equivalent performance results for the total (H) and the four energy intervals (EI) (t=thermal, < 0.414 eV; s=slow, 0.414 eV - 0.1 MeV; m=medium, 0.1 - 1 MeV; f=fast, 1 - 12 MeV) for the *insitu* and source spectra. The values depicted were obtained by dividing the measured dose equivalent by the reference value for both the EIs and the total (Tables 1 and 2).

The CPND provided exceptional total H results and reasonable spectrometric results. However, a slight spectral inaccuracy was exhibited in the region between 0.01 and 1 MeV. Improving the resolution in this region, corresponding to the area of greatest change in  $h_p$ , would provide improved spectral accuracy which would in turn facilitate superior total neutron dose equivalent accuracy. CANS is being developed with the goal of obtaining this sought-after spectral resolution. The advantages of CANS over the CPND may be found in 1) the modification of the TLD component, eliminating the need for a phantom, providing greater thermal neutron measuring accuracy and simulating a  $4\pi$  geometry, 2) the re-characterization of the energy response characteristics or response functions ( $R(E)$ ) of several previously considered BDs in hopes of obtaining better spectral resolution, and 3) assessing the temperature affects on the shape of the  $R(E)$  and how to correct for it. A miniature version of CANS, the Personal Neutron Dosimeter/Spectrometer (PENDOSE), is anticipated for personnel applications.

## OBSTACLES STILL REMAINING

There exist three obstacles which continue to impede the practical application of this technology: 1) an in-depth understanding of the effect of  $R(E)$  and spectrum on the response, i.e., the spectral nexus, 2) a low cost reader, and 3) conquering the temperature-dependent characteristics of the BD.

### Spectral Nexus

The application of calibration factors to correct for the difference in the  $R(E)$  of the dosimeter ( $R(E)$ ) and the  $h_p$  and the accompanying differences between the calibration and field spectra is a common practice. But the accuracy of such applications is only as good as the accuracy of the  $R(E)$  and the knowledge of the spectrum. Therefore, understanding the relationship between the response of the dosimeter and the shape of the spectra, or as we have defined it, the spectral nexus, is critical to performing good dosimetry. To understand the spectral nexus, we must understand the nexus between three separate elements: 1) the  $R(E)$  of our dosimeter, 2) the difference between the  $R(E)$  and the  $h_p$  curve, and 3) the energy distribution or shape of the spectrum of interest.

### *Response function, $R(E)$*

The  $R(E)$ s of the BD-100R and BDS-1500 emerged from the principal analysis of data originating from two independent studies. Both studies subjected BD-100Rs to mono-energetic neutrons obtained from accelerator-induced scattering reactions. One was conducted at the Pacific Northwest Laboratory (PNL), the other at the National Physical Laboratory (NPL) (Schwartz and Hunt 1991; Liu et al. 1989). The  $R(E)$ s were derived from fits to this data which were normalized to reflect a 1 bubble / 0.01 mSv (1 bu / mrem) response when irradiated to  $^{238}\text{PuBe}$ , (a BTI calibration source at Chalk River) (Buckner et al. 1991). Thus the  $R(E)$  is defined as the true response as function of incident neutron energy, in bu  $\text{cm}^2$ , of a 1 bu / 0.01 mSv BD.

### *Spectral shape and response*

The irradiation of the BD-100R to various neutron spectra has revealed a variation in the number of bubbles produced per mSv when receiving the same dose equivalent (Ipe et al. 1988); i.e., the  $R(E)$  is not identical to the  $h_p$  curve. This is seen by comparison of the  $R(E)$  and  $h_p$  curve (see Figure 3). The  $R(E)$  of the BD-100R and BDS-1500 were folded into reference spectra for five radioisotopic neutron sources available at DOSAR:  $^{238}\text{PuBe}$ ,  $^{241}\text{AmBe}$  and  $^{252}\text{Cf}$  unmoderated and moderated by  $\text{D}_2\text{O}$  and polyethylene ( $^{252}\text{Cf}_{(\text{PE})}$ ) to obtain source specific sensitivities in bu / 0.01 mSv (bu/mrem). The reference spectra were obtained either from published literature (Block et al. 1967; ISO/DIS 1986) or BMS measurements. The results are presented in Table 3.

The impact of spectral shape on response may be seen from a comparison of two spectra, unmoderated  $^{252}\text{Cf}$  and  $^{238}\text{PuBe}$ . Both have been normalized to reflect a 0.01 mSv spectrum after application of  $h_{\phi}$ . These have been superimposed on the  $R(E)_{100R}$  and  $h_{\phi}$  to help visualize the impact (see Figure 4). Inspection of the spectra reveals that the unmoderated  $^{252}\text{Cf}$  spectrum contains a greater number of neutrons in the flat segment of the BD-100R response curve than does the  $^{238}\text{PuBe}$  spectrum (both are 0.01 mSv spectra); ergo, there is a greater sensitivity (bu/mSv) to unmoderated  $^{252}\text{Cf}$  than  $^{238}\text{PuBe}$ . This spectral nexus exists for all neutron measuring devices and is proportional to the differences existing between the  $R(E)$  of the device and the  $h_{\phi}$ . The question becomes; How well do we know the  $R(E)$  of our devices and the spectrum of our neutron fields (particularly, for devices sensitive to low energy neutrons, the region below 100 keV)?

### Low cost reader

If you are considering the purchase of a bubble detector reader, be prepared to pay about \$35K (the latest available figure on the current generation bubble reader from BTI). At that price, the system should do everything but feed the dog and do laundry, right? Well, even this advanced reader requires a significant amount of operator interaction for selection of enhancement options and adjustment of thresholds (a critical parameter, we might add). Items which would improve the usefulness of the reader would be the ability to verifiably link a bubble count with a specific BD reading after the fact, the imaging of the bubbles instead of a bright spot of reflected/refracted light corresponding to bubbles, and storage of the image on hard disk making future retrieval and analysis at a later date possible (as with a TLD glow-curve). These advancements have been achieved in a reader developed for research at DOSAR.

Utilizing an old video camera, an existing PC-AT, some lamp parts and an off-the-shelf video analysis software system, we assembled a reader that all of you do-it-yourselfers will love, and for approximately one tenth the cost (video digitizing board and software for under \$3.5K). By virtue of varied lighting techniques, a ring-like image is achieved which more closely resembles a bubble. Thus, an image also containing the serial number of the BD is stored to disk for future retrieval and image processing. Provided in the software are a plethora of enhancement techniques that make this combination a potent research tool for those of us on a tight budget. Automation is also achievable via a macro feature making possible incorporation of a series of image enhancement techniques to achieve the desired resolution of the image, and an algorithm to perform discrimination and counting.

### Temperature Effects

The effect of temperature on the response characteristics of the BD must be carefully considered. The increase in response associated with an increase in temperature is attributable to 1) the sensitivity increase in the region above the threshold or knee (the knee being the point below which a dramatic decrease in response is observed, ideally 100 keV and 1,500 keV for the BD-100R and BDS-1500) and 2) an increase in the degree of superheat of the liquid thereby lowering the critical energy required for bubble formation effectively increasing the probability of bubble formation by neutrons to which it was previously "insensitive" at a lower temperature. This is reflected by a shifting of the  $R(E)$  "knee" downward.

Let us illustrate the second mode of sensitivity increase first. Consider the home run hitting abilities of a baseball team when playing at home (a factor of the distance the player can hit the ball and the distance to the fence). If we assume the pitcher to be a constant in this analogy, then the frequency of home runs for the team when playing away would be expected to increase when playing an opponent whose home field was smaller, i.e., a shorter distance to the fence. Those players who would just miss hitting it out at home would be more likely to hit one out on the smaller field, while the number of home runs hit by those players normally hitting it out at home would increase only slightly. This makes sense for bubble detectors if we consider the normal home run hitters in our analogy to be representative of the neutrons above the knee, those with a high probability of inducing bubble formation at the calibration temperature, and the occasional

home run hitters as neutrons just below the knee, while still capable of occasionally causing a bubble to form the probability is much lower. Increasing the temperature has the same effect on bubble formation as does playing on a field with a shorter distance to the fence. Those neutrons only occasionally causing a bubble to form at the calibration temperature (or at home) do so more often (with a much higher probability) at a higher temperature (on a shorter field).

During the previous mono-energetic irradiation experiments (Liu et al. 1989; Schwartz and Hunt 1990) the temperature varied by as much as 8°C. The best possible method of determining the correlation of temperature and energy would be to maintain one variable constant while varying the other. A new investigation is being proposed to assess the temperature affect on response by performing a series of mono-energetic irradiations while precisely controlling the temperature of the detectors. In this manner, the effect of temperature on the R(E) will be determined, i.e., the change in sensitivity at a specific energy as a function of temperature,  $\Delta R(E)dT$ . This work promises to make significant inroads toward a better understanding of BD response characteristics.

The first step in the procedure will be to determine the R(E) at a specified calibration temperature, i.e., 25°C. Next, the R(E) of each component is segmented into a number of defined energy intervals (EIs) with the sensitivity for each EI (R(EI)), taken to be the average sensitivity, in bu-cm<sup>2</sup>, in that region. The effective change in sensitivity per °C for each interval will be assessed from the data. Translated; instead of applying a single temperature correction for the change in sensitivity over the entire R(E), (the equivalent of assuming the shape of the R(E) is constant and only the amplitude or sensitivity changes, which we have seen is an incorrect assumption) we will correct for the temperature effects by reestablishing the shape of the R(E) to reflect what the R(E) would be at the irradiation temperature. Because the response of a BD is dependent upon the R(E) and the spectrum (the occasion for the source specific sensitivities) and that temperature changes cause changes in the R(E), correctly compensating for temperature would require derivation of a temperature correction factor for each spectrum. Therefore this method of compensating for the change in the shape of the R(E) attributable to temperature will provide a result that is inherently more correct than application of a single factor to the total number of bubbles produced.

#### *Application to CANS*

This newly acquired knowledge allows us to make more accurate measurements of neutron spectra at temperatures other than those at which the R(E) had been defined by redefining the R(E) of the BD at the irradiation temperature. The process could be as follows: 1) the temperature at the time of irradiation is recorded, 2) a tube correction coefficient, TCC, is applied to the response each BD to mimic the response of a 1 bu/0.01 mSv calibrated detector (analogous to applying an element correction coefficient method to individual TLD element readings), 3) the R(EI) matrix is modified to reflect the R(E) at the irradiation temperature, 4) the matrix is inverted producing equations for the fluence represented in each EI,  $\phi_{EI}$  as a function of the TCC correction response of each component BD, 5) the TCC values are inserted and the equations solved to yield the  $\phi_{EI}$ , 6) application of the averaged  $h_{\bullet}$  for each EI provides the neutron dose equivalent contributed in that EI,  $H_{EI}$ , and 7) the summation of these reflects the total neutron dose equivalent measured.

The performance of CANS is anticipated to be at least as good as that demonstrated by the CPND and promises better resolution in the 0.01 to 1 MeV region and better correction for temperature dependence. Attractive assets of CANS include: 1) the fact that neutron fluence, a real quantity, is the foundation for determining the neutron dose equivalent, 2) that there is only a single solution to the algorithm matrix and 3) that only one algorithm is necessary regardless of the spectra. Note also, that these steps are easily automated via spreadsheet and microcomputer.

## HOPE FOR THE FUTURE

The payoff for all that has been invested will be a proven application of this technology. Yet, our vision is the incorporation of all we have learned into development of a real-time neutron spectrometer/dosimeter. An alternative real-time acoustical processing technique (ARAP), currently under development at DOSAR, may hold the key to unlocking the passageway which leads to realization of a real time application of BD technology. With the current availability of miniaturized stand-alone  $\mu$ -processors, the marriage of this and ARAP could transport BD application into the era of high-tech. By providing a measure of fluence and dose equivalent in real time it will answer the clarion call for a simple device for determining neutron spectra and dose equivalent. In our mind's eye the devices resemble those of the artist conception in Figures 5 and 6.

## REFERENCES

- Block, S., Bryan, J., Prevo, C. and Montan, D. *Laboratory sources enhanced in 0.5 eV to 200 keV neutrons for instrument evaluation*. Health Phys. 13:1025-1031, 1967.
- Buckner, M. A., Sims, C. S. and Miller, L. F. *Improving Neutron Dosimetry Using Bubble Detector Technology*. to be published as ORNL TM-11916 (in draft).
- Glaser, D. A. *Some Effects of Ionizing Radiation on the Formation of Bubbles in Liquids*. Phys. Rev. **87**, 665 (1952).
- International Commission on Radiological Protection. *Data for Protection Against Ionizing Radiation for External Sources*. (Oxford: Pergamon Press) ICRP Publication 21 (1973).
- Ipe, N. E. and Busick, D. D. *BD-100: The Chalk River Nuclear Laboratories' Neutron Bubble Detector*. Stanford University, SLAC-PUB-4398 Stanford, California, USA (1987).
- Ipe, N. E., Busick, D. D. and Pollock, R. W. *Factors Affecting the Response of the Bubble Detector BD-100 and a Comparison of its Response to CR-39*. Radiat. Prot. Dosim. **23**(1-4), 135-138 (1988).
- International Organization for Standardization. *Neutron reference radiations for calibrating neutron measuring devices used for radiation protection purposes and for determining their response as a function of neutron energy*. Geneva: ISO; Draft International Standard ISO/DIS 8529; 1986.
- Liu, J. C. *The Development, Characterization, and Performance Evaluation of a New Combination Type Personnel Neutron Dosimeter*. Ph.D. Dissertation, Texas A&M University, College Station, Texas (1989) (Also Oak Ridge National Laboratory, Oak Ridge, Tennessee 37831, ORNL-6593 (1989).
- Liu, J. C. and Sims, C. S. *Characterization of the Harshaw Albedo Tld and the Bubble Detectors BD-100R and BDS-1500*. Radiat. Prot. Dosim. **32**(1), 21-32 (1990).
- Liu, J. C. and Sims, C. S. *Performance Evaluation of a New Combination Personnel Neutron Dosimeter*. Radiat. Prot. Dosim. **32**(1), 33-43 (1990).
- Schwartz, R. B. and Hunt, J. B. *Measurement of the Energy Response of the Superheated Drop Neutron Detectors*. Radiat. Prot. Dosim. **34**(1), 377-380 (1990).

Table 1. Neutron  $H_{II}$  and  $H_T$  *in-situ* results of the CPND.

|       | GLOVE <sup>a</sup> |              | CAVE <sup>a</sup> |              | CNTRL <sup>a</sup> |              | WASTE <sup>a</sup> |              | LAB <sup>a</sup> |              |
|-------|--------------------|--------------|-------------------|--------------|--------------------|--------------|--------------------|--------------|------------------|--------------|
|       | CPND               | CPND\<br>REF | CPND              | CPND\<br>REF | CPND               | CPND\<br>REF | CPND               | CPND\<br>REF | CPND             | CPND\<br>REF |
| $H_I$ | 413.67             | 0.92         | 67.30             | 0.84         | 6.09               | 0.93         | 182.63             | 0.73         | 260.67           | 0.96         |
| $H_m$ | 202.98             | 0.82         | 65.46             | 1.15         | 4.53               | 1.43         | 184.64             | 1.34         | 143.25           | 0.94         |
| $H_s$ | 37.32              | 0.96         | 10.57             | 0.82         | 0.71               | 0.82         | 16.02              | 0.92         | 19.25            | 1.36         |
| $H_t$ | 20.34              | 0.85         | 15.11             | 1.31         | 0.33               | 9.43         | 3.16               | 0.75         | 1.25             | 5.86         |
| $H_T$ | 674.31             | 0.89         | 158.44            | 0.98         | 11.65              | 1.10         | 386.45             | 0.94         | 424.42           | 0.96         |

<sup>a</sup> Units = 0.1 mSv (mrem)

Table 2. Neutron  $H_{II}$  and  $H_T$  radioisotopic results of the CPND.

|       | <sup>252</sup> Cf <sub>(PE)</sub> <sup>a</sup> |              | <sup>238</sup> PuBe <sup>a</sup> |              | <sup>252</sup> Cf <sub>(D2O)</sub> <sup>a</sup> |              | MIX (2) <sup>a</sup> |              | MIX (3) <sup>a</sup> |              |
|-------|--|--------------|----------------------------------|--------------|---|--------------|----------------------|--------------|----------------------|--------------|
|       | CPND   | CPND\<br>REF | CPND                             | CPND\<br>REF | CPND  | CPND\<br>REF | CPND                 | CPND\<br>REF | CPND                 | CPND\<br>REF |
| $H_I$ | 46.30  | 0.82         | 56.47                            | 1.02         | 174.42  | 1.18         | 50.68                | 1.03         | 453.31               | 1.05         |
| $H_m$ | 31.77  | 1.67         | 6.76                             | 0.89         | 37.15   | 0.58         | 11.79                | 0.87         | 77.37                | 0.90         |
| $H_s$ | 2.40   | 0.70         | 0.19                             | 1.19         | 35.66   | 1.03         | 6.82                 | 1.21         | 8.85                 | 0.41         |
| $H_t$ | 4.56   | 1.06         | 0.09                             | 1.09         | 0   | 1            | 0.29                 | 1.29         | 2.14                 | 1.00         |
| $H_T$ | 85.03  | 1.02         | 63.51                            | 1.01         | 247.23  | 1.00         | 69.58                | 1.02         | 541.67               | 1.00         |

<sup>a</sup> Units = 0.1 mSv (mrem)

Table 3. Calculated radioisotopic source sensitivities.

| SOURCES               | <sup>252</sup> Cf <sub>(D2O)</sub> | <sup>252</sup> Cf <sub>unmod</sub> | <sup>241</sup> AmBe | <sup>238</sup> PuBe | <sup>252</sup> Cf <sub>(PE)</sub> |
|-----------------------|------------------------------------|------------------------------------|---------------------|---------------------|-----------------------------------|
| BD-100R <sup>a</sup>  | 0.97                               | 1.12                               | 0.94                | 1.00                | 1.09                              |
| BDS-1500 <sup>a</sup> | 0.73                               | 1.01                               | 0.98                | 1.00                | 0.72                              |

<sup>a</sup> Units = bubble / 0.01 mSv (bu mrem<sup>-1</sup>)

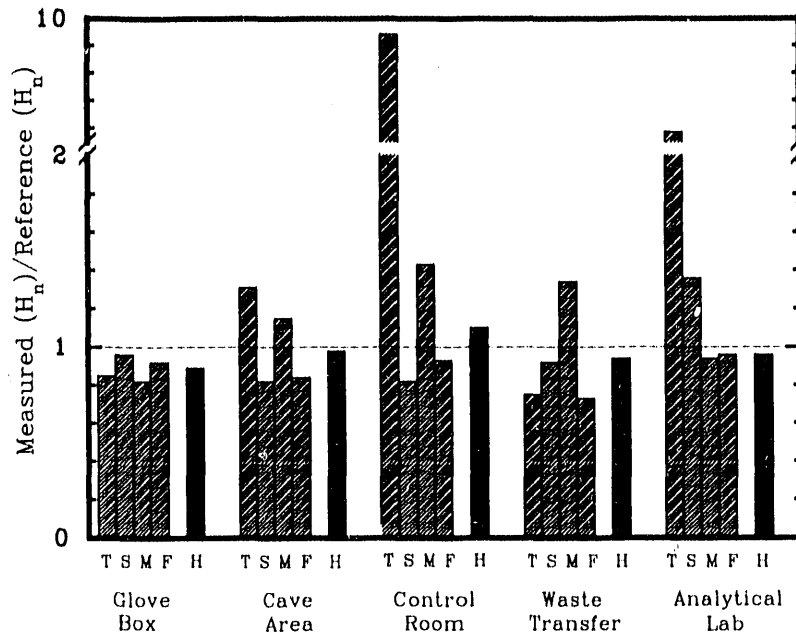


Fig. 1. The Relative accuracy of the CPND to measure neutron equivalent ( $H_{El}$  and  $H_T$ ) for ORNL field spectra at REDC.

T, S, M and F =  $H_{El}$  (measured)/ $H_{El}$  (reference).      H = total  $H_T$  (measured)/ $H_T$  (reference).

T = < 0.414 eV  
M = 0.1 - 1 MeV

S = 0.414 eV - 0.1 MeV  
F = 1 - 12 MeV

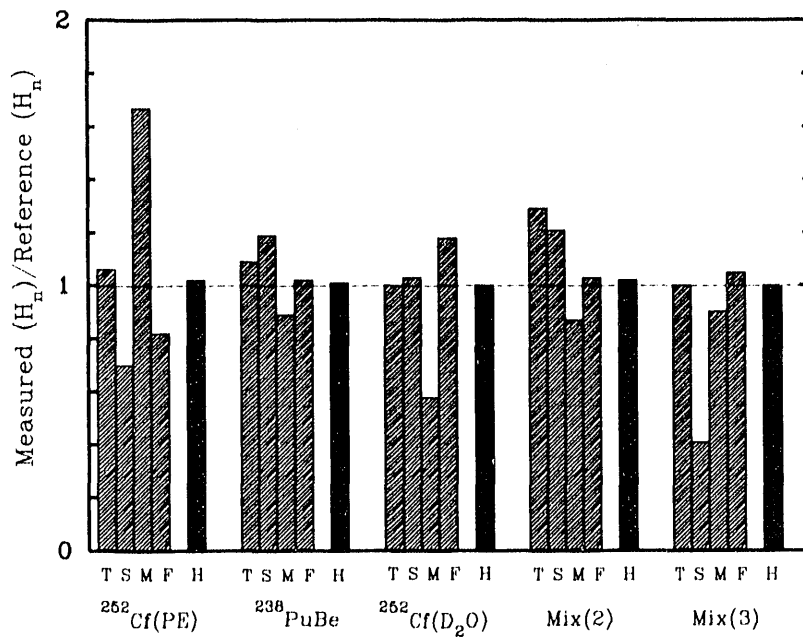


Fig. 2. The Relative accuracy of the CPND to measure neutron equivalent ( $H_{El}$  and  $H_T$ ) of RADCAL source spectra.



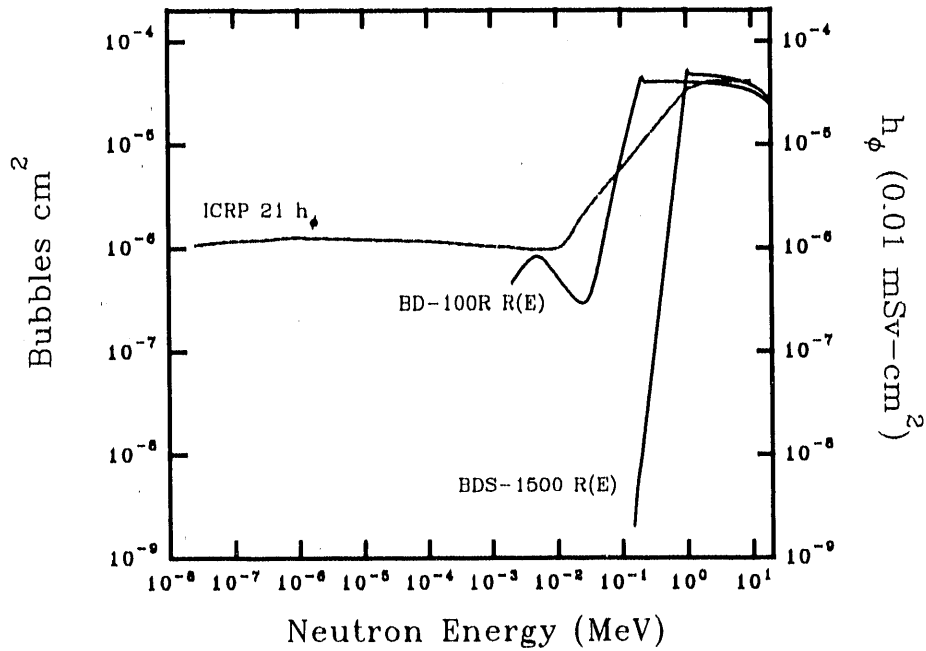


Fig. 3. Derived response function,  $R(E)$ , of the BD-100R and BDS-1500 and the ICRP  $h_\phi$  curve.

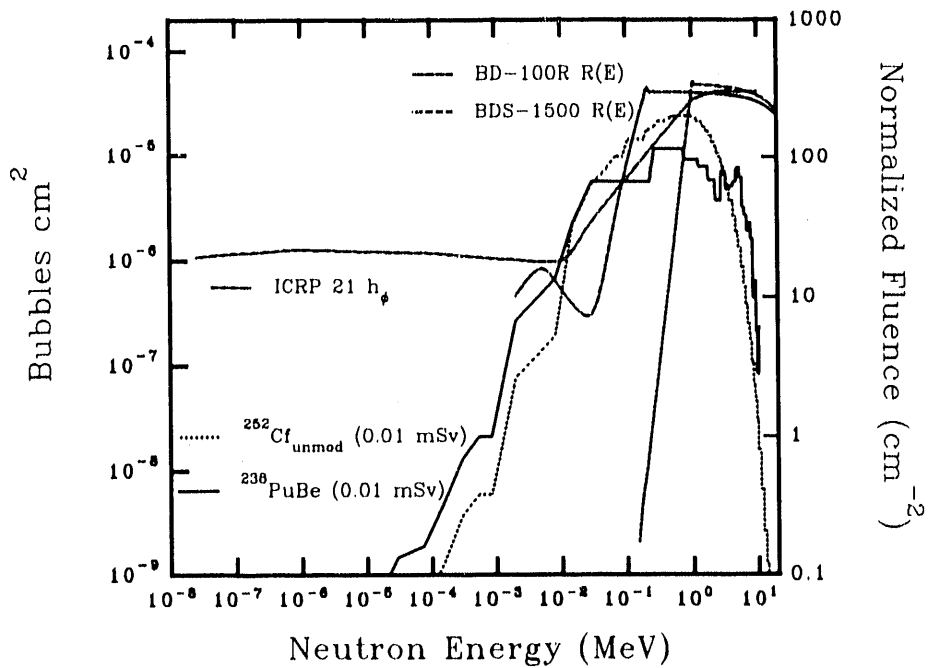


Fig. 4. Derived response function,  $R(E)$ , of the BD-100R and BDS-1500, the ICRP  $h_\phi$  and the 0.01 mSv (1 mrem)  $^{252}\text{Cf}_{\text{unmod}}$  and  $^{238}\text{PuBe}$  spectra.

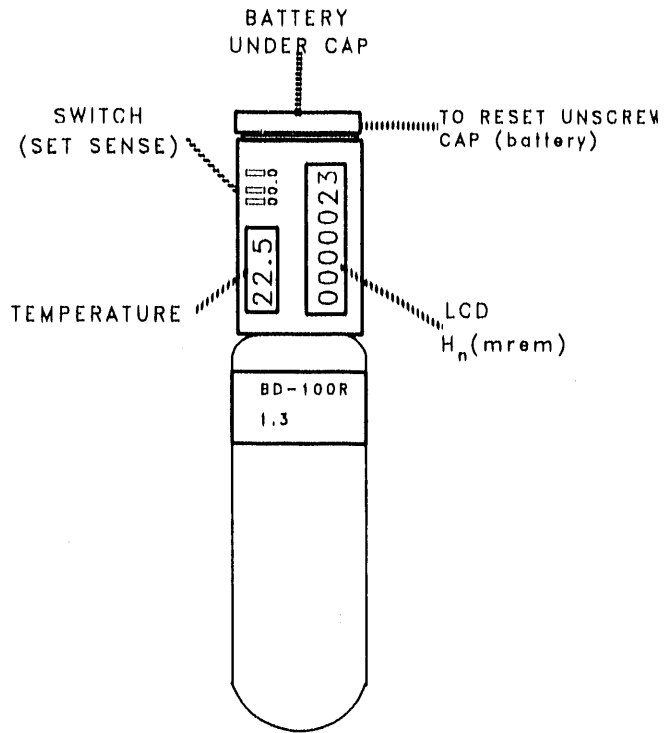


Fig. 5 The real time version of the BD-100R.

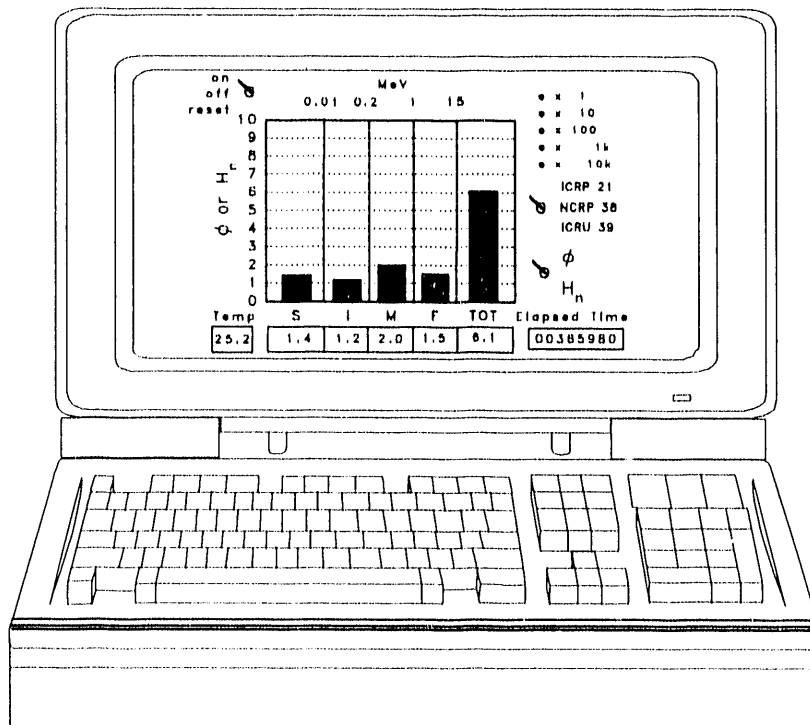


Fig. 6 Real time neutron spectrometer with graphical user interface; displays  $\phi$  or H for EIs and total; choice of desired  $h_n$ ; utilizes a 386 laptop.